Journal of Zhejiang University-SCIENCE A (Applied Physics & Engineering)
ISSN 1673-565X (Print); ISSN 1862-1775 (Online)
www.zju.edu.cn/jzus; www.springerlink.com
E-mail: jzus@zju.edu.cn

Theoretical analysis and experimental study of an air inflated membrane structure

Jing-hai GONG†, Xiu-ying YANG, Zi-zhao ZHANG, Jin-cheng ZHAO

(*Department of Civil Engineering, Shanghai Jiao Tong University, Shanghai 200240, China*)

†E-mail: gongjh@sjtu.edu.cn

Received Apr. 8, 2009; Revision accepted Aug. 31, 2009; Crosschecked Nov. 9, 2009

Abstract: In this paper, an experimental study of an air inflated membrane was carried out based on the China National Stadium (the Bird's Nest). After the 2008 Olympic Games, it was apparent that the future use of the Bird's Nest would be enhanced if rainfall could be prevented from entering the stadium. The installation of an air inflated membrane across the opening of the steel structure was proposed as a solution to this problem. To verify the scheme, a theoretical analysis and experimental study of an air inflated membrane was carried out. Experimental and computational models were developed, form-finding was carried out using both experimental and theoretical methods, and the results from the two approaches, including the deflection of the air inflated membrane and deformation of the support structure, were analyzed and compared. The force-transfer path and deformation of the air inflated membrane under loads was studied. Conclusions and suggestions are presented.

Key words: China National Stadium, Air inflated membrane, Form-finding
doi:10.1631/jzus.A0900127 **Document code:** A **CLC number:** TU3

1 Engineering background

1.1 Survey of the Bird's Nest

The China National Stadium, also known as the Bird's Nest (Fig. 1), is located in the central zone of the Olympic Park in Beijing. It was the main stadium for the 29th Olympic Games held in Beijing in 2008, and successfully hosted not only the opening and closing ceremonies but also the track and field events. The Bird's Nest occupies 20.4 hectares, with a construction area of 258 000 m^2. It has a saddle shape (elliptical hyperboloid) with a long axis of 332.3 m and a short axis of 297.3 m. The highest point of the Bird's Nest roof is 68.5 m, and the lowest point is 40.1 m. The opening in the middle of the roof is 185.3 m long and 127.5 m wide (CAG, 2006; Fan *et al.*, 2007).

1.2 Rain proofing of the Bird's Nest

After the Olympic Games, people began to consider the future use of the stadium. Covering the stadium to prevent rain entering was considered as one way of improving future usage. We propose a new scheme to install an air inflated membrane over the opening of the roof of the Bird's Nest to solve the rain proofing problem (Fig. 2). The advantages of an air inflated membrane include its light weight, large span, fast construction, easy disassembly and attractive appearance (Robinson-Gayle *et al.*, 2001; van Dessel *et al.*, 2003; Bell, 2008). An air inflated membrane roof can be used to provide shelter from rain, snow and burning sun, ensuring comfortable conditions for all kinds of activities, and thus has great practical significance and economic benefit.

2 Experimental approach

To validate the analysis of installing an air inflated membrane on the Bird's Nest, a 1:20 scale model was constructed and tested. The experimental approach was as follows:

(1) Analyze and compare the form-finding result of the air inflated membrane.

(2) Research the mechanical behavior and the load bearing capacity of the air inflated membrane under uniform loads and their influence on the support truss.

(a)

(b)

Fig. 1 Steel structure of the China National Stadium
(a) Elevation; (b) Bird view

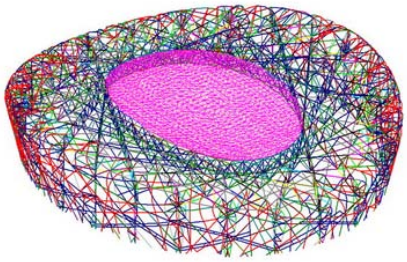

(a)

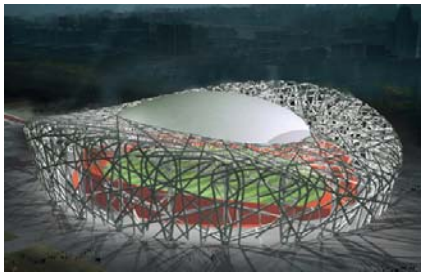

(b)

Fig. 2 Steel structure combined with an air inflated membrane. (a) Analysis model; (b) Render map

(3) Observe the deformation and mechanical performance of the air inflated membrane under local concentrated loads.

(4) Compare experimental data with theoretical results, to validate the theoretical analysis.

(5) Discuss possible explanations for differences between experimental and theoretical results and identify issues requiring more attention in practice.

(6) Investigate the process of construction and installation of the air inflated membrane.

3 Experimental model

3.1 Design of the experimental model

A 1:20 scale model of the air inflated membrane supported by a steel truss was used in the test. The air inflated membrane was an elliptical hyperboloid 9.12 m long, 6.2 m wide, and 1.362 m high. Its projective area was 44.6 m^2. The mesh spacings of cables were about 0.55 m, and the initial air pressure was 0.3 kPa. The prestressed force of the upper cables was 0.6 kN and that of the bottom cables was 0.75 kN. The diameter of all cables was 5 mm, the section area was 19.63 mm^2, and the prestressed force of the membrane in both warp and fill was 0.5 kN/m. The form-finding result from theoretical analysis (Gong, and Qiu, 2002; Kim and Lee, 2002; Bletzinger *et al.*, 2005) is shown in Fig. 3, and the experimental model is shown in Fig. 4.

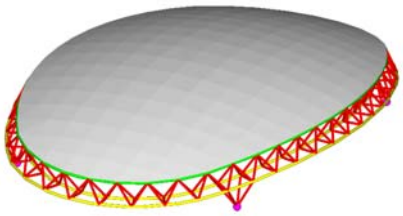

Fig. 3 The form-finding result

Fig. 4 The experimental model

A tubular steel truss was used as the supporting structure (Fig. 4), which simulated the inner edge of the roof of the Bird's Nest. The influence of the air inflated membrane on the supporting structure could be analyzed (Li and Chan, 2004; Hegyi *et al.*, 2006; Kerdid *et al.*, 2008). The section of the upper and bottom chords of the truss was Φ60 mm×3.5 mm, and that of the connecting rod on the bottom chord, the web members, and the members on abutment was Φ48 mm×3 mm.

3.2 Conformation of the experimental model

Fig. 5 shows a photograph of the cable anchors connecting with the steel structures. There is a hinge connection at the end of each cable, which allowed the cable to rotate in the vertical plane, and the direction of the cable anchor could be adjusted during the gas charging and load application process of the air inflated membrane. The length of the cable could be modified using a button in the cable anchor to adjust the prestressed force.

Fig. 5 Anchor device at cable end

3.3 Analysis model and software

Cable-membrane analysis software (SMCAD) developed by the authors was used to analyze the experimental model. A nonlinear finite element method was used in form-finding analysis and load analysis of the air inflated membrane structure (Bonet *et al.*, 2000; Gil and Bonet, 2006; 2007). In the finite element analysis, 2-node cable elements and triangle membrane elements were used, and a beam element was used in the steel structure. As usual, the nodes deflections were presumed to be coupled between cable elements and membrane elements in the cable-membrane structure computational model. However, this did not correspond to the real condition. The contact condition between the cables and the membrane was very complex in the experimental model (Fig. 6). Friction existed between the cables and the membrane, relative deflection appeared under loads, and the cables were even separated from the membrane in localized areas.

Fig. 6 Contact of cable and membrane

4 Experimental schemes

4.1 Measuring points

Displacement sensors and strain gauges were arranged in each quarter of the model according to the symmetry of the whole model. The displacement sensors of the supporting truss were set at each end of both the long and the short axes (Fig. 7): points 1 and 3 measured horizontal deformation, points 2 and 4 measured vertical deformation. Fig. 8 shows the positions of the strain gauges on the cable anchors: odd numbers measured the upper cables and even numbers measured the bottom cables. Deflection measuring points of the bottom layer membrane are shown in Fig. 9.

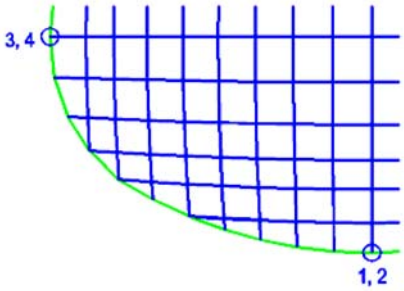

Fig. 7 Position of displacement sensors

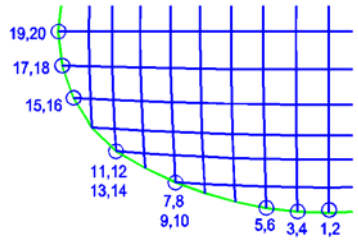

Fig. 8 Position of strain gauges

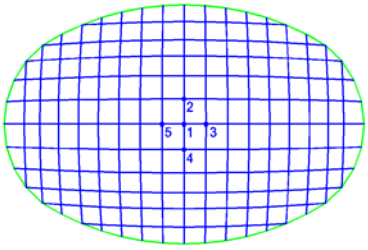

Fig. 9 Deflection measuring points of the bottom layer membrane

4.2 Loading schemes

The loads on the air inflated membrane are expected to come mainly from snow, wind, and other local live loads such as construction, examination and repair, maintenance loads, etc. Because a wind load is very difficult to simulate, the mechanical behavior of the air inflated membrane and the supporting truss were studied mainly under snow load in the test. The deformation of the air inflated membrane under local concentrated load was also studied.

Sandbags were used to simulate snow loads in the test and were applied at two weights: 0.1 and 0.3 kN/m^2. The sandbags spread out when placed on the air inflated membrane, and simulated a uniform snow load quite well. Each sandbag weighed 0.15 kN and so a total of 33 sandbags were used to simulate a snow load of 0.1 kN/m^2 and 99 for a snow load of 0.3 kN/m^2.

A local concentrated load was simulated directly by some students standing on the model, which accords with the practical condition.

5 Model test

5.1 Form-finding test

In the form-finding test, the air inflated membrane was charged with gas using an air pump until the air pressure reached the pre-determined value, then test results, such as the shape of the model and the tension of the upper and bottom cables, were obtained and compared with the theoretically computed results.

The initial air pressure of the experimental membrane was 0.3 kPa. Figs. 3 and 4 show the form-finding results from theoretical analysis and the test. The shapes of the two models were very similar. The thickness of the air inflated membrane was calculated by measuring the elevations of the central points on the upper and lower layers of the membrane. Table 1 lists the thickness from the test and from theoretical analysis.

Table 1 Form-finding results of the air inflated membrane (unit: m)

	Test results	Computational results
Elevation of the upper layer membrane center	1.604	1.549
Elevation of the bottom layer membrane center	0.246	0.389
Thickness	1.358	1.160

The test thickness was larger than that of the computational result (Table 1). This was caused mainly by the original design of the membrane which did not achieve the expected result. Because of a lack of experience in designing and processing air inflated membranes, the membrane was cut according to the chord axis of the theoretical supporting truss in the original design (Fig. 10a). We expected that because the planar projection of the membrane was bigger than the opening of the supporting truss, the edge of the air inflated membrane would contact the chord and cover the opening (Fig. 10b). However, in practice, this did not happen: the membrane did not touch the chord at all after it was inflated, and there was a large gap between them (Fig. 10c). By analysis, we know that the reason for the membrane model not being the expected shape is that the diameter of the supporting truss was too small, only 60 mm. The experimental model was modified to correspond to the computational model.

Another reason was that the assembly precision of the supporting truss was not sufficiently accurate. The membrane model was first assembled in the factory, thus precision was ensured. However, because the model was too big to be transported

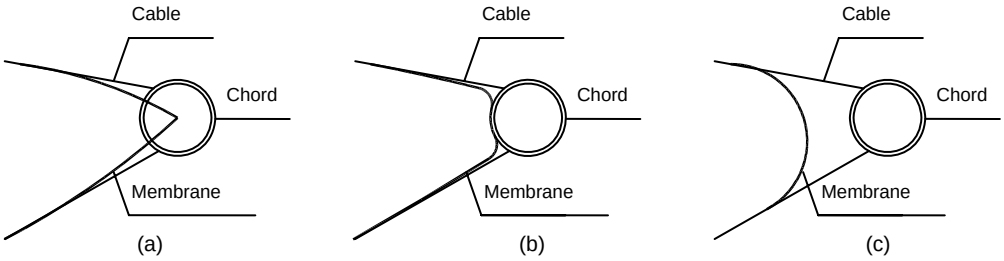

Fig. 10 Sketch of the membrane edge
(a) Form-finding result; (b) Expected result; (c) Actual result

integrally, the supporting truss had to be divided into four segments and reassembled in the laboratory. Restricted by the experimental conditions, the precision of the truss reassembly could not be ensured adequately.

5.2 Uniform load test

5.2.1 Loading

Firstly, the air inflated membrane was inflated until the inner pressure reached 0.3 kPa, while the data from the strain gauge transducer, displacement transducer, and the deformation of the membrane were recorded as the initial conditions of the analysis. Then the sandbags were placed on the membrane in two separate tests to simulate uniform snow loads of 0.1 and 0.3 kN/m^2 (Fig. 11), and the results were recorded. Finally, the model was unloaded completely, and the final results recorded.

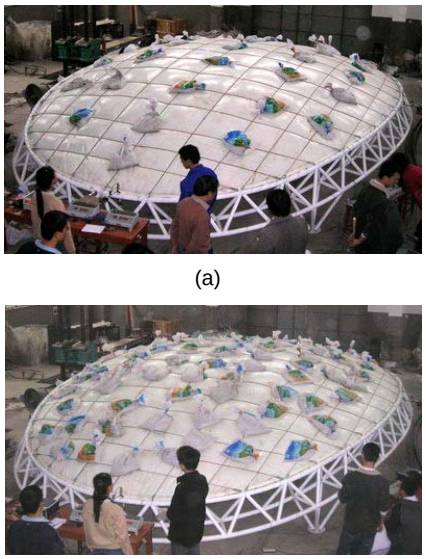

(a)

(b)

Fig. 11 Load case 1 (0.1 kN/m^2) (a) and load case 2 (0.3 kN/m^2) (b)

5.5.2 Inner air pressure of the membrane

A comparison between the inner air pressure as measured by testing and from computational results, is shown in Table 2.

Table 2 The inner air pressure (unit: kPa)

	Initial state	0.1 kN/m^2 load	0.3 kN/m^2 load	Unloading
Test data	0.30	0.41	0.59	0.30
Computational results	0.30	0.42	0.57	0.30
Difference (%)	0	2.40	−3.40	0

Before discussing the variation in the inner air pressure, it is necessary to explain the air tightness of the air inflated membrane. Only a membrane with adequate air tightness can ensure a favorable working condition. Modification of the experimental model caused air leakage from the membrane. A test of air leakage was carried out. The initial air pressure was 0.3 kPa, which decreased to about 0.28 kPa one hour later and to about 0.1 kPa after 24 h. The loading time was about one hour, so we deduced that the inner pressure loss caused by air leakage was about 0.02 kPa during the test. As the inner pressure returned to 0.3 kPa after unloading, it seemed that there was no loss of inner pressure. However, in fact, the air leak was serious and the inner pressure loss was more than 0.02 kPa, because the inner pressure increases during the loading process. The return of the inner pressure to 0.3 kPa was caused by the temperature of the inner air rising, which can be explained by two reasons: the temperature of the whole laboratory increased during the test, and heat was generated in the inner air during the loading process.

The changes in membrane inner air pressure and volume with increasing temperature were analyzed.

The inner air pressure increased by about 0.04 kPa with an increase in temperature of 1 °C (Fig. 12a). The inner air volume increased by about 0.1 m^3 with an increase in temperature of 1 °C (Fig. 12b). So the influence of temperature on the mechanical behavior of the air inflated membrane must be taken into account.

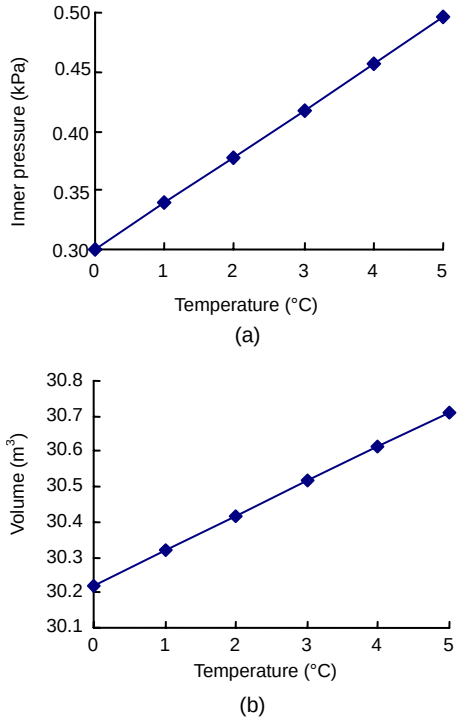

Fig. 12 Curve of (a) inner pressure and (b) volume with temperature

The test data agree well with the computational results. The differences between them are only 2.4% with a load of 0.1 kN/m^2 and −3.4% with a load of 0.3 kN/m^2. Considering the influence of air leakage and temperature variation, the theoretical results can predict the change in membrane inner air pressure under loads. Inner air pressure is a very important index in mechanical analysis of air inflated membranes. The experimental results validate the computational method adopted in this study and the corresponding computational results.

5.2.3 Deflection of the air inflated membrane

The deflections of five points on the bottom layer membrane were measured (Fig. 9), and also computed using the finite element method (Levy *et al.*, 2004; Woo *et al.*, 2004; Jarasjarungkiat *et al.*, 2008; 2009). The results of experiment and computation are compared in Table 3.

The data showed the expected response to the two weight loadings, but the changes in the test result data were generally much higher than those in the computational data. The average differences between them were −14.1% for the 0.1 kN/m^2 load and −40.5% for the 0.3 kN/m^2 load.

5.2.4 Deflection of the supporting truss

The test data for deflections of the four points on each of the ends of the supporting truss (Fig. 7) were compared with the computational results (Table 4).

Table 3 The deflections of the bottom layer membrane (unit: mm)

No.	0.1 kN/m^2 load			0.3 kN/m^2 load		
	Test data	Computational results	Difference (%)	Test data	Computational results	Difference (%)
1	−2	−4.93	146.5	−15	−12.44	−17.1
2	−8	−4.76	−40.5	−28	−12.05	−57.0
3	−4	−4.80	20.0	−19	−12.39	−34.8
4	−6	−4.76	−20.7	−21	−12.05	−42.6
5	−8	−4.80	−40.0	−20	−12.39	−38.1
Average	−5.6	−4.81	−14.1	−20.6	−12.26	−40.5

Table 4 The deflections at the ends of the support truss (unit: mm)

No.	0.1 kN/m^2 load			0.3 kN/m^2 load		
	Test data	Computational results	Difference (%)	Test data	Computational results	Difference (%)
1	−0.54	−0.90	66.7	−2.57	−2.46	−4.3
2	0.35	0.11	−68.6	0.83	0.54	−34.9
3	0.38	0.44	15.7	1.21	1.19	−1.6
4	−0.36	−0.73	102.8	−1.52	−2.20	44.7

Nos. 1 and 3 in Table 4 are horizontal deflections. The positive values mean outward deflection and the negative values mean inward deflection. Nos. 2 and 4 are vertical deflections. The positive values mean upward deflection and the negative values mean downward deflection. The computational results predicted the deflection direction at the ends of the long axis and the short axis of the supporting truss. The computational result data of the horizontal deflection were similar to the test data, the largest difference being only 4.3% when the load was 0.3 kN/m^2. The difference in vertical deflection was larger, which was caused mainly by the uneven prestressed force of the cables and the difference between the actual supporting condition and its assumption.

5.2.5 Reasons for differences between theoretical analysis and experimental results

The main reasons for differences between theoretical analysis and experimental results from uniform loads tests were as follows. First, the form-finding results of the experimental membrane differed from those of the computational result. The experimental model had to be modified, and the modification was difficult to incorporate into the loading analysis. Second, restricted by the experimental condition, the precision of the truss reassembly in the laboratory could not be ensured. Last, the deformations of the cables and the membrane were presumed to be the same at the connections in the computational model, which is different from the real condition. The relationship between the cables and the membrane relates to the contact connection problem, and this has not been solved very well in the analysis of the actual cable-membrane structure.

5.2.6 Mechanical behavior of the air inflated membrane

Under a snow or live load, the upper layer of the air inflated membrane deforms downward and the stresses on the upper cables and membrane decrease, the volume of the inner air decreases accordingly and the inner air pressure increases. Thus, the loads are transferred to the bottom layer, the bottom layer of the air inflated membrane deforms downward, and the stresses on the bottom cables and membrane increase, then the loads are finally transferred to the supporting truss. In contrast, under wind suction, the upper layer deforms upward and the stresses on the upper cables and membrane increase, the volume increases accordingly and the inner air pressure decreases, so the bottom layer deforms upward and the stresses on the bottom cables and membrane decrease.

5.3 Local concentrated load test

Local concentrated load tests were carried out to determine whether the air inflated membrane had enough bearing capacity and rigidity under local concentrated load, and whether the whole structure retained its shape. The local concentrated loads were simulated by some students standing on the membrane. Their positions are shown in Fig. 13.

(a)

(b)

Fig. 13 Local concentrated load. (a) Loads concentrated; (b) Loads scattered

Under the local concentrated loads (Fig. 13), the air inflated membrane had good bearing capability and retained a favorable shape. There were local deformations on the surface of the membrane at the positions where the students were standing. After unloading the local concentrated loads, the air inflated membrane restored its original shape.

6 Conclusions and suggestions

Based on the theoretical analysis and experimental study of the air inflated membrane structure, the following conclusions can be drawn and suggestions made.

1. Tests on an air inflated membrane were described in this paper, and data relating to changes in the mechanical behavior and deformation of the membrane structure under loads were obtained. Although there were differences between the experimental results and the theoretical analysis, the test results in general reflected the predicted behavior of the air inflated membrane under loads. The test data matched the theoretical results mostly, and the differences could be explained by logical reasons, so the experimental objectives were achieved.

2. Gong *et al.* (2009) analyzed and compared in detail the expected mechanical behavior of the Bird's Nest steel structure before and after installation of the air inflated membrane. The installation of an air inflated membrane across the opening region of the Bird's Nest to solve the rain proofing problem has the possibility of implementation.

3. During the analysis process of the whole model of the air inflated membrane and the supporting truss, we encountered the problem of "small numbers cover with big numbers" during the iteration. The stiffness of the cables and the membrane was far smaller than that of the supporting truss, causing the iteration cannot converge. To ensure the feasibility of the whole model analysis, better computational methods have been adopted to control the iterative convergence.

4. Temperature has a great influence on the inner air pressure and the volume of the air inflated membrane, and must be taken into account in the analysis.

5. When the model or the practical project of the air inflated membrane is being produced, the variation in length of the cables and the membrane caused by the conformation of the joints and the construction error should be modified, otherwise the form-finding result and mechanical behavior will be greatly affected. The membrane material should be hot-cohered compactly to guarantee the air inflated membrane has the desired air tightness; air leakage can make the air inflated membrane lose rigidity and bearing capacity.

6. The membrane is too heavy in practice for people to pull onto the cable meshes in air inflated membrane projects, so mechanical equipment should be designed to retract the membrane. A reasonable air pump number, pump power, and wire diameter should be calculated according to the volume of inner air and the expected air inflation time. It is difficult to deflate the inner air completely. This needs to be considered in the design of membrane retracting equipment.

References

Bell, L., 2008. Pneumatic Membrane Structures for Space and Terrestrial Applications. Proceedings of the 11th International Conference on Engineering, Science, Construction, and Operations in Challenging Environments, Long Beach, California, USA, p.1-8. [doi:10.1061/40988(323)109]

Bletzinger, K.U., Wuchner, R., Daoud, F., Camprubi, N., 2005. Computational methods for form finding and optimization of shells and membranes. *Computer Methods in Applied Mechanics and Engineering*, **194**(30-33):3438-3452. [doi:10.1016/j.cma.2004.12.026]

Bonet, J., Wood, R.D., Mahaney, J., Heywood, P., 2000. Finite element analysis of air supported membrane structures. *Computer Methods in Applied Mechanics and Engineering*, **190**(5-7):579-595. [doi:10.1016/S0045-7825(99)00428-4]

China Architecture Design & Research Group (CAG), 2006. The Total Explication of Steel Structure Design in China National Stadium. China Architecture Design & Research Group, Beijing, China (in Chinese).

Fan, Z., Liu, X.M., Fan, X.W., 2007. Design and research of large-span steel structure for the National Stadium. *Journal of Building Structures*, **28**(2):1-16 (in Chinese).

Gil, A.J., Bonet, J., 2006. Finite element analysis of prestressed structural membranes. *Finite Elements in Analysis and Design*, **42**(8-9):683-697. [doi:10.1016/j.finel.2005.10.009]

Gil, A.J., Bonet, J., 2007. Finite element analysis of partly wrinkled reinforced prestressed membranes. *Computational Mechanics*, **40**(3):595-615. [doi:10.1007/s00466-006-0129-7]

Gong, J.H., Qiu, G.Z., 2002. Computer Aided Design of Space Structure. China Architecture & Building Press, Beijing, China, p.173-195 (in Chinese).

Gong, J.H., Yang, X.Y., Zhang, Z.Z., Zhao, J.C., 2009. Feasibility Study for the Application of Air Inflated Membrane Structure in China National Stadium. *Journal of Shanghai Jiao Tong University (Science)*, **14**(1):76-80. [doi:10.1007/s12204-009-0076-5]

Hegyi, D., Sajtos, I., Geiszter, G., Hincz, K., 2006. Eight-node quadrilateral double-curved surface element for membrane analysis. *Computers and Structures*, **84**(31-32):2151-2158. [doi:10.1016/j.compstruc.2006.08.046]

Jarasjarungkiat, A., Wuchner, R., Bletzinger, K.U., 2008. A

wrinkling model based on material modification for isotropic and orthotropic membranes. *Computer Methods in Applied Mechanics and Engineering*, **197**(6-8):773-788. [doi:10.1016/j.cma.2007.09.005]

Jarasjarungkiat, A., Wuchner, R., Bletzinger, K.U., 2009. Efficient sub-grid scale modeling of membrane wrinkling by a projection method. *Computer Methods in Applied Mechanics and Engineering*, **198**(9-12):1097-1116. [doi:10.1016/j.cma.2008.11.014]

Kerdid, N., le Dret, H., Saïdi, A., 2008. Numerical approximation for a non-linear membrane problem. *International Journal of Non-Linear Mechanics*, **43**(9):908-914. [doi:10.1016/j.ijnonlinmec.2008.06.007]

Kim, J.Y., Lee, J.B., 2002. A new technique for optimum cutting pattern generation of membrane structures. *Engineering Structures*, **24**(6):745-756. [doi:10.1016/S0141-0296(02)00003-2]

Levy, R., Chen, C.S., Lin, C.W., Yang, Y.B., 2004. Geometric stiffness of membranes using symbolic algebra. *Engineering Structures*, **26**(6):759-767. [doi:10.1016/j.engstruct.2003.12.011]

Li, J.J., Chan, S.L., 2004. An integrated analysis of membrane structures with flexible supporting frames. *Finite Elements in Analysis and Design*, **40**(5-6):529-540. [doi:10.1016/S0168-874X(03)00076-3]

Robinson-Gayle, S., Kolokotroni, M., Cripps, A., Tanno, S., 2001. ETFE foil cushions in roofs and atria. *Construction and Building Materials*, **15**(7):323-327. [doi:10.1016/S0950-0618(01)00013-7]

van Dessel, S., Chini, A.R., Messac, A., 2003. Feasibility of rigidified inflatable structures for housing. *Journal of Architectural Engineering*, **9**(1):1-10. [doi:10.1061/(ASCE)1076-0431(2003)9:1(1)]

Woo, K., Igawa, H., Jenkins, C.H., 2004. Analysis of wrinkling behavior of anisotropic membrane. *Computer Modeling in Engineering and Sciences*, **6**(4):397-408.